

# An XPS study of hexagonal polyoxymethylene with various bulk morphologies: surface modification under X-ray exposure

P. Boulanger‡, J. Rigat‡, J. Delhalle§ and J. J. Verbist‡

‡Laboratoire de Spectroscopie Electronique, §Laboratoire de Chimie Théorique Appliquée, Facultés Universitaires Notre-Dame de la Paix, 61 rue de Bruxelles, B-5000 Namur, Belgium

(Received 11 February 1987; revised 24 August 1987; accepted 3 November 1987)

A comparative study of hexagonal polyoxymethylene with various bulk morphologies, supported by differential scanning calorimetry (d.s.c.) and infra-red attenuated total reflectance (i.r.-a.t.r.) spectroscopy, is made by X-ray photoelectron spectroscopy (XPS). Both core and valence levels are analysed providing evidence for surface degradation of the polymer under XPS conditions.

(Keywords: POM; valence band; degradation)

## INTRODUCTION

The macromolecular chains of highly crystalline polyoxymethylene (POM) samples may exist in two different conformational states. The energetically most stable form is a 9/5 helix which crystallizes in the hexagonal system<sup>1</sup>, with a torsional angle of 78° around the C–O bond, whereas the orthorhombic form<sup>2</sup> presents a 2/1 helical conformation (torsional angle 63.7°) and is stable only at temperatures below 60°C and pressures lower than 1 atmosphere. In a previous paper<sup>3</sup>, quantum mechanical calculations performed on simple model molecules predicted a slight influence of the chain conformation on the shape of the theoretically simulated valence band spectra. Experimental work is in progress to verify these predicted modifications, due mainly to the different torsional angles around the C–O bonds described above.

However, before studying the influence of such structural effects on the XPS signals, it is essential to check the modifications at the surface due to exposure to monochromatized X-rays (i.e. free of high energy Bremsstrahlung) during XPS data acquisition.

It is well known that the morphology at the surface influences the degradation resistance: for example in the case of the chemical etching<sup>4</sup>, we have recorded the XPS core level peaks and valence band spectra of several hexagonal POM samples, differing in their degree of crystallinity, orientation of the crystalline zones, and lamellar or fibrillar nature. Differential scanning calorimetry (d.s.c.) and infra-red total attenuated reflectance (i.r.-a.t.r.) spectroscopy measurements were made on the samples prior to XPS recordings in order to monitor the bulk characteristics.

## EXPERIMENTAL

### Sample preparation

All the samples (see Table 1) were used as received without any recrystallisation or purification. Only Delrin 100 was gently scraped to remove the observed surface hydrocarbon contamination.

### Differential scanning calorimetry (d.s.c.)

The melting behaviour of the samples was examined on a Perkin-Elmer DSC-2 apparatus. The heating rate was 10°C min<sup>-1</sup> and the sample weight was about 5 mg. The temperature and heat of fusion were calibrated with indium (429.8 K, 6.97 cal g<sup>-1</sup>). In order to avoid dependence of the results on experimental conditions (sample weight, heating rate etc.)<sup>7</sup>, the melting temperature was taken as the intersection with the horizontal (temperature) axis of the tangent to the increasing side of the melting peak, at the inflexion point.

### Infra-red attenuated total reflectance (i.r.-a.t.r.) spectroscopy

I.r.-a.t.r. spectra were obtained on a Perkin-Elmer 850 apparatus equipped with a variable angle internal reflection attachment in the sampling compartment. For the measurement, a KRS-5 crystal with an incidence angle of 45° was used in such a way that the penetration depth is about 0.29  $\lambda$  (2–3  $\mu\text{m}$ ) for the region concerned (1500–1000 cm<sup>-1</sup>)<sup>8</sup>.

### XPS measurements

The photoelectron spectra were recorded on a Hewlett-Packard 5950A ESCA spectrometer using

monochromatized Al K $\alpha$  radiation ( $h\nu = 1486.6$  eV). The sample was irradiated in a vacuum chamber (pressure below  $10^{-8}$  Torr) while cooled with liquid nitrogen down to 283 K. Because of the insulating properties of the polymer, the surface charge effect was controlled by the use of an electron flood-gun whose current ( $I < 1$  mA) and energy ( $E < 4$  eV) were adjusted to neutralize surface electrostatic charges. Calibration of the spectra was done by mixing the polymer with a reference compound, polyethylene, for which the C<sub>1s</sub> level energy was fixed at 284.6 eV. A valence band spectrum recording requires an overnight accumulation and is recognized to be satisfactory when at least two similar spectra are obtained on similar samples.

## RESULTS

### Bulk characteristics

Through information from crystallinity studies and melting behaviour available in the literature, the bulk morphology of the samples can be well characterized (Table 2). However, as the crystallinity content was determined by different methods in different cases, a homogeneous classification of the samples (following their degree of crystallinity) requires further d.s.c. measurements. The crystallinity content is calculated from the formula:

$$\% \text{Crys} = (\Delta H / \Delta H_f) \times 100$$

where  $\Delta H$  is the heat of fusion of the studied sample and  $\Delta H_f$  is the heat of fusion of the single crystal. In the case of POM,  $\Delta H_f$  was chosen equal to  $2.35 \text{ kcal mol}^{-1}$  (ref. 9).

Unfortunately, this method is only approximate because it does not take into account additional effects such as the length of crystallites. Moreover, it suffers from the difficulty in resolving the melting and degradation peaks, which almost overlap for needle-like extended chain crystals. Nevertheless, the melting temperatures

and the heats of fusion of the various samples presented in Table 2 support the morphological structure established in the same table.

POM needle-like crystalline polymers (II) have the highest melting temperature,  $186^\circ\text{C}$ . POM samples (I, III) with rather wide melting peaks and lowest melting temperatures present typical behaviour of semicrystalline polymers. When Delrin 100 (III) is submitted to microwave heat drawing, its melting peak becomes sharp and moves to higher temperatures (from  $170$  to  $182^\circ\text{C}$ ). Meanwhile, the crystallinity increases to  $77\%$ , as previously reported<sup>6</sup>, because of the orientation of the fibrils along the drawing direction followed by crystallisation of the amorphous regions. This is confirmed by the i.r.-a.t.r. spectra (Figure 1), when considering the  $1300\text{--}500 \text{ cm}^{-1}$  region. There is a strong decrease of the crystallinity-dependent band at  $1140 \text{ cm}^{-1}$ , accompanied by an increase of the band at  $935 \text{ cm}^{-1}$ . Following the observations of Shimomura and Iguchi<sup>10</sup> on several samples of various crystallinities, the

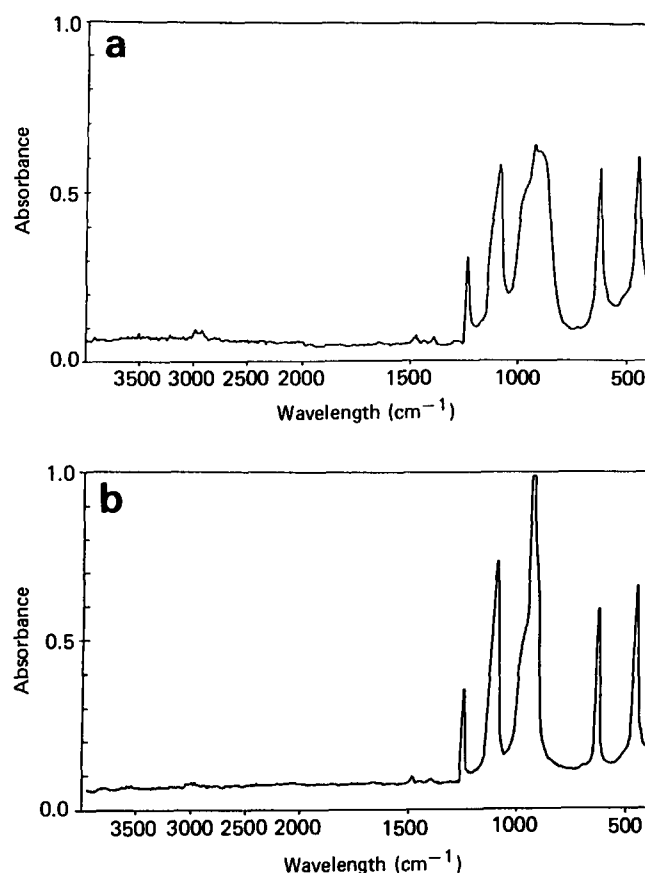


Figure 1 I.r.-a.t.r. spectra of Delrin 100: (a) undrawn sample; (b) sample drawn under microwave heating

Table 1 Description of hexagonal polyoxymethylene samples used in this work

POM sample	Morphological appearance	$M_n$	Source
(I) Delrin 500 NC 10	Powder	157 000	du Pont de Nemours
(II) Needle-like, BF <sub>3</sub> etched	Light powder	125 000	Dr M. Iguchi <sup>5</sup>
(III) Delrin 100, undrawn	Tapes	66 000	Dr K. Nakagawa <sup>6</sup>
(IV) Delrin 100, drawn (draw ratio = 29)	Tapes	66 000	id

Table 2 Morphology, crystallinity and melting temperature of hexagonal polyoxymethylene samples used in this work

Sample	Crystallinity (%)	Morphology	$\Delta H$ (kcal mol <sup>-1</sup> ) (this work)	D.s.c. crystallinity (%) (this work)	Melting point (°C) (this work)
(I)	69 (X-ray) <sup>18</sup>	Semicrystalline	1.77	75.0	168
(II)	100 (X-ray) <sup>17</sup>	Single crystals needle shaped	—	—	186
(III)	84* (pulsed n.m.r.) <sup>6</sup>	Semicrystalline	1.69	72.0	170
(IV)	95* (id)	Oriented semicrystalline	1.81	77.0	182

\*Volume crystallinity.

attenuation of the band at  $1140\text{ cm}^{-1}$  confirms the high degree of crystallinity of the drawn polymers and the disappearance of the irregular structures of the amorphous regions, while the peak at  $900\text{ cm}^{-1}$ , characteristic of the regular structure<sup>10,11</sup> of the helical

conformation is slightly increased. The increase of the crystallinity-independent peak at  $935\text{ cm}^{-1}$  is due to the reinforced interaction between the polarized i.r.-a.t.r. beam and the C–O–C symmetric stretching mode<sup>12</sup>: the medium has become more anisotropic after drawing and the electric field vector points perpendicularly to the direction of elongation.

#### X-ray photoelectron spectra

**Core levels.** For the  $-(\text{CH}_2-\text{O})-$  unit, the values of the  $\text{C}_{1s}$  and  $\text{O}_{1s}$  binding energies, respectively 287.8 eV (see peak A, Figure 2) and 532.9 eV, are identical to those previously observed for POM<sup>13</sup>.

As reported in Table 3, all the starting samples contain a slight degree of hydrocarbon contamination ( $\text{C}_{1s}$  peak D at 284.6 eV). After an overnight exposure to the X-ray beam, this peak is increased and broadened, from 1.2 to 1.6 eV, due mainly to the contribution of two additional  $\text{C}_{1s}$  components, B and C respectively, at 284.8 and 285.9 eV. These energy levels are characteristic of carbon signals from  $-(\text{CH}_2-\text{CH}_2-\text{C}^a\text{H}_2-\text{C}^b\text{H}_2-\text{O})-$  segments. It is reasonable to think that some proportion of the exposed methoxy carbon is reduced in an alkyl form carbon. Indeed, in our case the total carbon content to oxygen ratio,  $\text{C}_T/\text{O}$  (Table 3) increases slightly and simultaneously the 'a'-type carbon vs. oxygen intensity ratio,  $\text{O}-\text{C}^a-\text{O}/\text{O}$ , decreases under the action of the X-ray beam on the POM samples.

Sample (II) of highest crystallinity seems to be the most sensitive to radiation damage.

This phenomenon, well known in heavy metals compounds, and reported here for the first time in the case of such oxygenated polymeric materials, would consist mostly in a chemical reduction due to interaction with the electrons emitted by the sample under irradiation rather than a heating effect due to the X-ray beam. This is supported by the sensitivity of the samples to an electron beam: severe and rapid cracking damage is observed when the Delrin 100 POM is exposed to the scanning electron microscopy beam<sup>14</sup> (Figure 3).

In the case of suitable polymers, the same technique is able to give much more precise information on the structure of the chains at the surface, e.g. orientation of the benzene groups at the surface of methylene styrene copolymers<sup>15</sup> has been determined. Recently, Gardella *et al.*<sup>4</sup> have been able to relate surface inhomogeneities to folded chains when considering poly(tetramethyl *p*-siloxane) at various degrees of crystallinity.

In the case of POM, structural information such as the depth profile of the reduced polymer are quite difficult to obtain from core level peak analysis.

Accordingly, it seems reasonable to attempt to trace the degradation in the valence band spectrum region of higher sampling depth, typically  $90\text{ \AA}$ <sup>15</sup>.

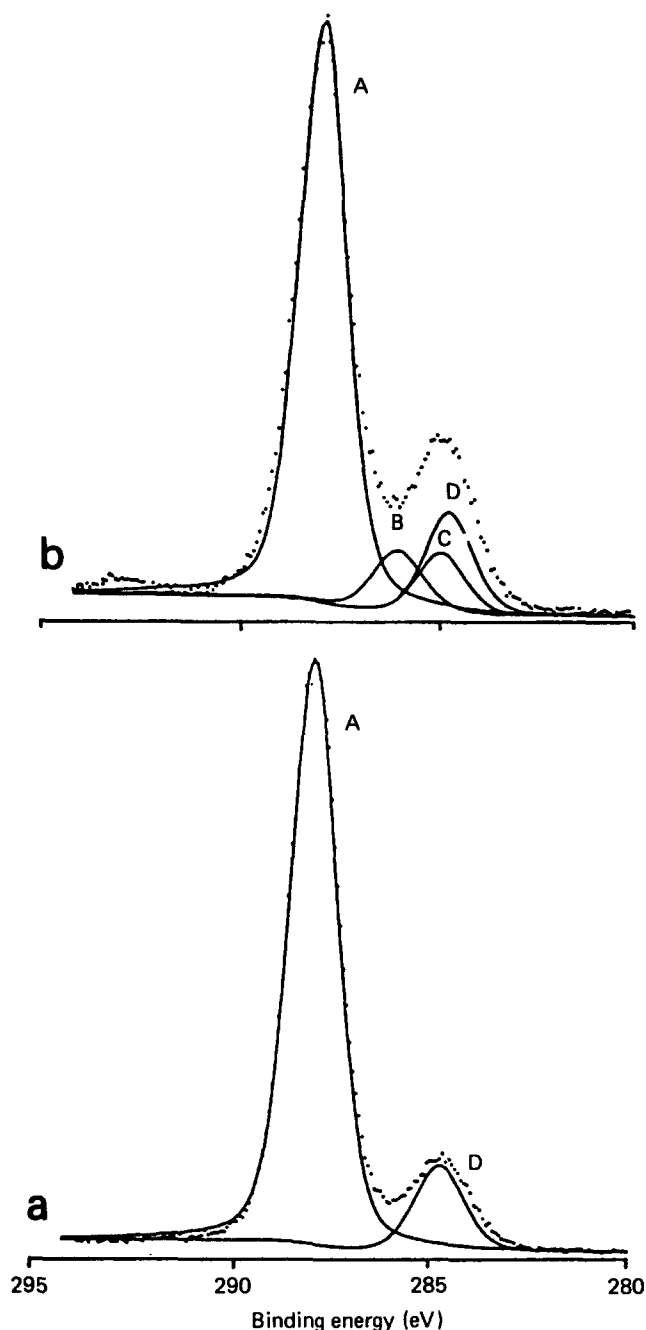


**Figure 2**  $\text{C}_{1s}$  core level spectra of POM needle-like  $\text{BF}_3$  etched: (a) before the recording of the valence band; (b) after recording of the valence band

**Table 3** XPS  $\text{C}_{1s}/\text{O}_{1s}$  intensity ratios in hexagonal POM samples: total carbon ( $\text{C}_T$ ), methoxy carbon and hydrocarbon impurities (hc) and reduction products (rp)

Sample	Before exposure			After exposure		
	$\text{C}_T/\text{O}$	$\text{O}-\text{C}^a-\text{O}/\text{O}$	hc (%)	$\text{C}_T/\text{O}$	$\text{O}-\text{C}^a-\text{O}/\text{O}$	hc + rp (%)
(I)	0.42 (0.02)*	0.40 (0.02)	3.5	0.50 (0.01)	0.36 (0.01)	17.0
(II)	0.42 (0.04)	0.39 (0.03)	6.0	0.51 (0.08)	0.36 (0.02)	19.0
(III)	0.42 (0.01)	0.40 (0.01)	5.0	0.44 (0.01)	0.37 (0.01)	16.0
(IV)	0.39 (0.01)	0.37 (0.01)	3.0	0.43 (0.02)	0.38 (0.01)	15.0

\* Values in parentheses are the standard deviations

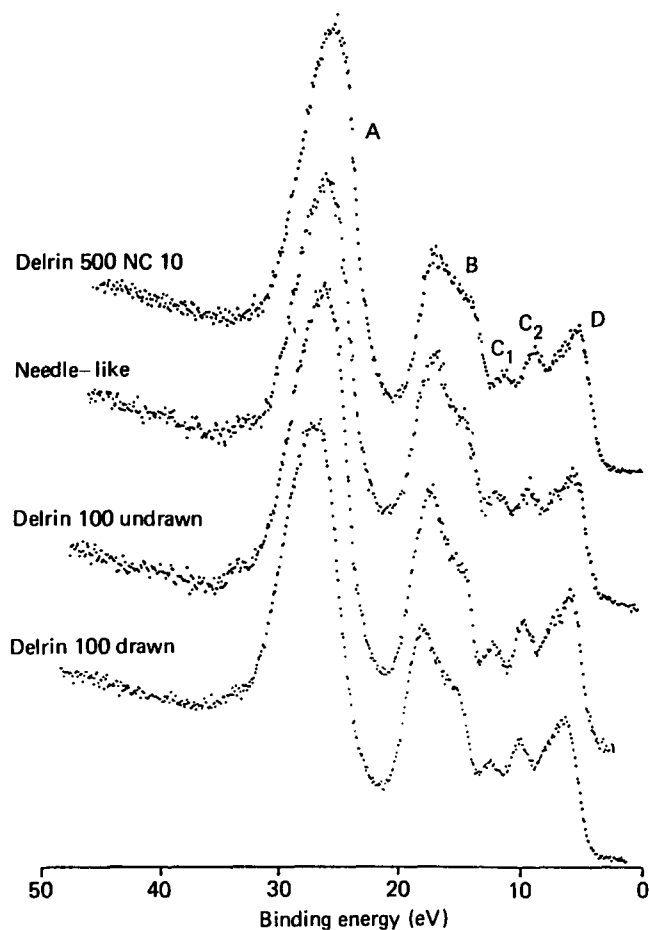


Figure 3 XPS valence band spectra of hexagonal POM

**Valence bands.** Valence band spectra of the four POM hexagonal samples are shown in Figure 4. All the spectra present five maxima at about 26.7 eV (A), 17.6 eV (B), 12.0 eV (C1), 9.6 eV (C2) and 6.0 eV (D) (Table 4). The two peaks of lowest energy, A and B, are attributed to states with, respectively, dominant  $O_{2s}$  (26.7 eV) and  $O_{2s}-C_{2s}$  (17.6 eV) contribution. Peak D of lowest binding energy (6.0 eV) is characteristic of the  $C_{2p}-O_{2p}$  combination. The intermediate weak bands, C<sub>1</sub> and C<sub>2</sub>, (9.6–12.0 eV) are characteristic of the carbon–hydrogen valence interactions where the  $C_{2p}$  character is dominant.

All the valence band spectra look identical, except for that of Delrin 500 NC 10, where the 17.6 eV band (B) vs. the  $O_{2s}$  band (A) intensity ratio is reduced. Moreover, the four spectra are in perfect agreement with the theoretical valence band spectrum of hexagonal POM<sup>3</sup>.

From previous work, the valence band spectrum has proved to be sensitive to modifications in the secondary structure of polymers such as polyethylene which are stable to X-ray exposure<sup>16</sup>.

Recently, theoretical calculations performed on folded alkane model molecules demonstrated that such structural changes affect the valence band structure<sup>17</sup>. Similarly, the influence of the conformational characteristics of the POM chains on the shape of their valence band spectrum has been predicted theoretically<sup>3</sup>: a slight modification of the torsional angle from 78 to 63.7°C of the chain induces a broadening and a shift of the highest energy peak from 9.49 to 9.69 eV.

Accordingly, structural modifications at a depth sampled by the valence band photoelectrons may be detected in the valence band spectrum. However,

although the degradation shows slightly different intensities for the samples, their valence band spectra do not differ significantly and are in perfect agreement with the theoretical spectrum, as already mentioned.

It is thus reasonable to consider that the reduction phenomenon occurs in the top layers near the sample surface in such a way that the contribution of undegraded POM will be the most important in the valence band. The observed spectra can be considered as the valence band of pure POM, with some admixture of polytetrahydrofuran as impurity.

CONCLUSION

X-ray photoelectron spectroscopy appears to be a very sensitive tool for the investigation of chemical modifications occurring at the surface of some polymeric

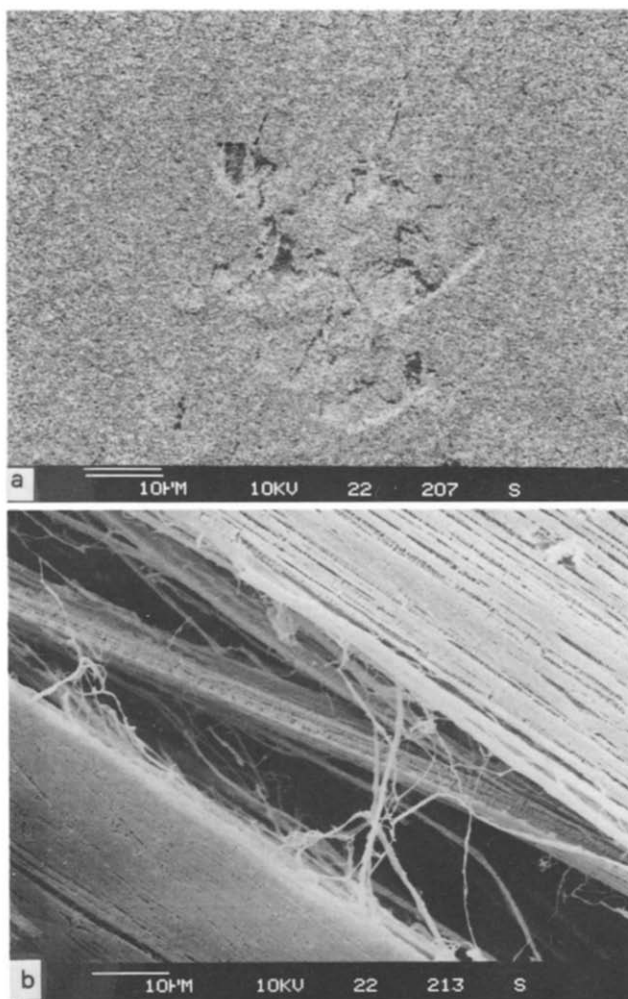


Figure 4 Scanning electron microscope views of POM Delrin 100 after a few seconds exposure to the electron beam: (a) undrawn sample; (b) drawn sample

Table 4 XPS valence peak positions for hexagonal POM samples

Sample	Binding energy ( $\Delta E \pm 0.1$ eV)				
	$O_{2s}$	$O_{2s}-C_{2s}$	$C_{2p}-H_{1s}$	$C_{2p}-O_{2p}$	
	A	B	C1	C2	D
(I)	26.5	17.7	11.9	9.6	5.8
(II)	26.7	17.6	12.3	9.7	6.0
(III)	26.6	17.5	12.1	9.5	5.8
(IV)	26.6	17.7	12.0	9.7	6.0

materials during the measurements; core level and valence band spectra provide complementary information.

#### ACKNOWLEDGEMENTS

We are very grateful to Dr M. Iguchi, Research Institute on Polymers and Textiles, Japan, for providing POM samples with a high crystallinity, and to Dr K. Nakagawa, Nippon Telegraph and Telephone Corporation, Ibaraki Electrical Communications Laboratories, Japan, for supplying the drawn POM samples. POM Delrin 500 NC 10 was supplied by du Pont de Nemours. The d.s.c. and i.r.-a.t.r. measurements were performed in the Laboratoire des Hauts Polymères, Catholic University of Louvain-la-Neuve, Belgium, and we thank Dr R. Legras for his collaboration.

#### REFERENCES

- 1 Takahashi, Y. and Tadokoro, H. *J. Polym. Sci., Polym. Phys. Edn.* 1978, **17**, 123
- 2 Carazzolo, G. and Mammi, M. *J. Polym. Sci. (A)* 1963, **1**, 965; Iguchi, M. *Polymer* 1983, **24**, 915
- 3 Boulanger, P., Lazzaroni, R., Verbist, J. and Delhalle, J. *Chem. Phys. Lett.* 1986, **129**, 275
- 4 Gardella, J. A., Jr, Chen, J. S., Magill, J. H. and Hercules, D. M. *J. Am. Chem. Soc.* 1983, **105**, 4536
- 5 Iguchi, M. *Br. Polym. J.* 1973, **5**, 807
- 6 Takeuchi, Y., Yamamoto, F., Nakagawa, K. and Yamakawa, S. *J. Polym. Sci., Polym. Phys. Edn.* 1985, **23**, 1193
- 7 Iguchi, M. *Makromol. Chem.* 1976, **177**, 549
- 8 Harrick, N. J. 'Internal Reflectance Spectroscopy', Wiley Interscience, New York, 1967
- 9 Suzuki, H., Grebowicz, J. and Wunderlich, B. *Makromol. Chem.* 1985, **186**, 1109
- 10 Shimomura, M. and Iguchi, M. *Polymer* 1982, **23**, 509
- 11 Terlemezian, L., Mihailov, M., Schmidt, P. and Schneider, B. *Makromol. Chem.* 1978, **179**, 807
- 12 Tadokoro, H., Kobayashi, M., Kawaguchi, Y., Kobayashi, A. and Murahashi, S. *J. Chem. Phys.* 1963, **38**, 703
- 13 Dilks, A. *Anal. Chem.* 1981, **53**, 802A
- 14 Zihlif, A. M. *Mat. Chem. Phys.* 1985, **13**, 21
- 15 Dilks, A. in 'Electron Spectroscopy: Theory, Techniques and Applications', (Eds C. R. Brundle and A. D. Baker), Academic Press, London, 1981, Vol. 4, p. 279
- 16 Pireaux, J. J., Riga, J., Caudano, R. and Verbist, J. J. *ACS Symp. Ser.* 1981, **162**, 169
- 17 Delhalle, J., Delhalle, S. and Riga, J. *J. Chem. Soc., Faraday Trans. 2*, 1987, **83**, 503
- 18 Iguchi, M. and Murase, M. *J. Crystal Growth* 1974, **24/25**, 596
- 19 Iguchi, M., Kanetsuna, H. and Kawai, T. *Makromol. Chem.* 1969, **128**, 63